Numerical Investigation of Liquid Flow in Two-, Three- and Four-Stage Centrifugal Pumps

Nicolas La Roche-Carrier, Guyh Dituba Ngoma and Walid Ghie
University of Quebec in Abitibi-Témiscamingue, School of Engineering's Department, 445, Boulevard de l'Université, Rouyn-Noranda, Quebec, J9X 5E4, Canada

Keywords: Centrifugal Pump, Multistage, Impeller, Diffuser, Computational Fluid Dynamics (CFD), Modeling and Simulation.

Abstract: In this study, a liquid flow in two-, three- and four-stage centrifugal pumps was numerical investigated. The continuity and Navier-Stokes equations with the k-ε turbulence model and standard wall functions were used by means of the ANSYS-CFX code. To enhance the design of the multistage pump, the impacts of the number of impeller blades, diffuser return vanes and the number of stages on the performances of a multistage centrifugal pump were analyzed. The results obtained demonstrate that the selected parameters affect the pump head, brake horsepower and efficiency in a strong yet different manner. To validate the model developed, the results of the numerical simulations were compared with the experimental results from the pump manufacturer.

1 INTRODUCTION

Multistage centrifugal pumps are widely used in industrial and mining enterprises (Peng W., 2008). For a more performing multistage pump, its design parameters, such as the number of stages, impeller blades, diffuser vanes and diffuser return vanes, angle of the impeller blade, height of the impeller blade and diffuser vane, the width of the impeller blade and diffuser vane, the impeller and diffuser diameter, the rotating speed of the impeller and the casing geometry must be determined accurately. Many experimental and numerical studies have been conducted on the liquid flow through a multistage centrifugal pump (Huang S. et al., 2006; Miyano M. et al., 2006; Kawashima D. et al., 2008; Gantar M. et al., 2002), where Huang S. et al., 2006 had numerically simulated using a CFD code a three-dimensional turbulent flow through an entire stage of a multistage centrifugal pump, including flows in a rotating impeller and stationary diffuser. They had found that the reverse flows existed near the impeller outlet, resulting in the flow field being asymmetric and unstable. There was considerable interference on the velocity field at the impeller exit because of the interaction between the impeller blades and diffuser vanes. Additionally, Miyano M. et al., 2006 had experimentally investigated the impacts of the return vane profile on the performances of the multistage centrifugal pump to optimize the stationary components in the multistage centrifugal pump. It was found, among other things, that the return vane, whose trailing edge was set at the outer wall radius of the downstream annular channel and discharged the swirl-less flow, had a positive impact on pump performances, while Kawashima D. et al., 2008 had experimentally investigated the impacts of the diffuser vane on the performances of the multistage centrifugal pump, accounting for the interactions among the diffuser vane, return vane and next stage impeller. In addition, Jirout T., 2014 had investigated the liquid flow in an agitated batch with pitched blade multi-stage impellers. Effects of various geometrical parameters of pitched blade multi-stage impellers on pumping ability have been analyzed. It was shown the impact of the distance between impellers in multi-stage configurations, on their pumping capacity and flow in the mixing bath in comparison with an independently operating pitched blade impeller with the same geometry. Furthermore, La Roche-Carrier et al., 2013 had numerically simulated the liquid flow in a first stage of a multistage centrifugal pump consisting of an impeller, diffuser with return vanes, and casing.

La Roche-Carrier N., Dituba Ngoma G. and Ghie W..
Numerical Investigation of Liquid Flow in Two-, Three- and Four-Stage Centrifugal Pumps.
DOI: 10.5220/0005096800920099
In *Proceedings of the 4th International Conference on Simulation and Modeling Methodologies, Technologies and Applications* (SIMULTECH-2014), pages 92-99
ISBN: 978-989-758-038-3

Effects of the impeller blade height and diffuser vane height, number of impeller blades, diffuser vanes and diffuser return vanes, and wall roughness height on the performances of the first stage of a multistage centrifugal pump were analyzed. Results of numerical simulations were compared with the experimental results from the pump manufacturer. Thorough analysis of previous works clearly demonstrated that the research results obtained are specific to the design parameters and configuration of the rotating and stationary components in single centrifugal pumps and multistage centrifugal pumps, and thus cannot always be generalized. Therefore, in this study, to enhance the design and performances of multistage centrifugal pumps as shown in Fig. 1 for example (Technosub inc.), accounting for the particularities of the geometry and configuration of the impeller and diffuser with return vanes, a numerical investigation was conducted using the ANSYS-CFX code (Ansys inc., 2011). This was done to gain further insight into the characteristics of the three-dimensional turbulent liquid flow through a multistage centrifugal pump while also considering various flow conditions and pump design parameters including the numbers of impeller blades (5, 6 and 7), the number of diffuser return vanes (3, 8, and 11), and the pump stage number (2, 3 and 4).

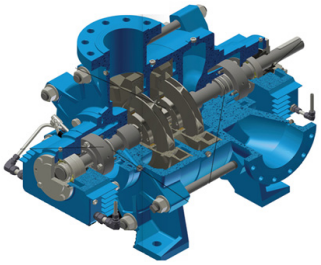

a) 2-stage centrifugal pump

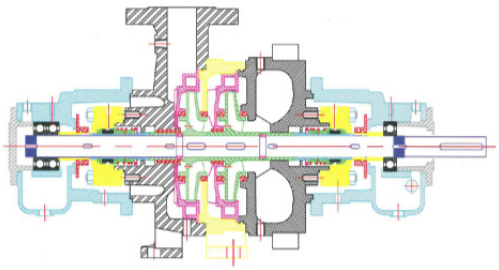

b) Cross-sectional view of 2-stage pump

Figure 1: Multistage centrifugal pump.

2 GOVERNING EQUATIONS

Fig. 2 shows the model of the first stage of a multistage centrifugal pump considered in this study. It consists of an impeller, diffuser with return vanes and casting.

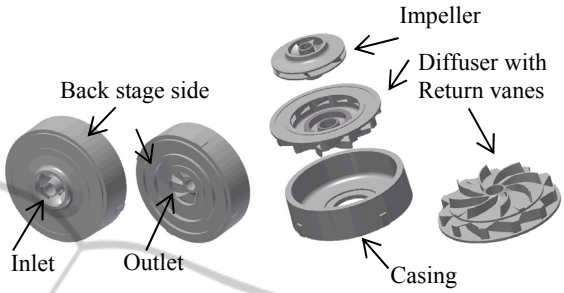

a) Pump stage b) Stage components

Figure 2: Model of centrifugal pump stage.

To run the numerical simulations, the used domain fluids of the impeller, diffuser with return vanes and the multistage centrifugal pumps (2-, 3-, and 4-stage) are shown in Fig 3.

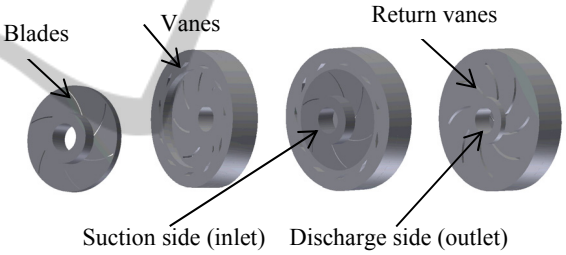

a) Impeller, diffuser and pump stage

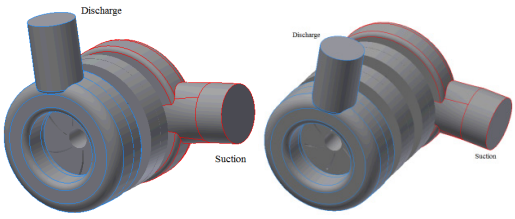

b) 2-stage c) 3-stage

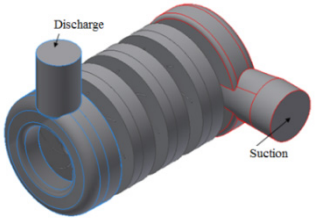

d) 4-stage

Figure 3: Domain fluids.

In the centrifugal pump stage's governing equations

for liquid flow, the following assumptions were made: (i) a steady state, three-dimensional and turbulence flow using the k-ε model was assumed; (ii) it was an incompressible liquid; (iii) it was a Newtonian liquid; and (iv) the liquid's thermophysical properties were constant with the temperature.

To account for these assumptions, the theoretical analysis of the liquid flow in the impeller passages, diffuser vane passages and diffuser return vane passages was based on the continuity and Navier-Stokes equations (Ansys inc., 2011). For the three-dimensional liquid flow through these components of a centrifugal pump stage as shown in Fig. 2, the continuity equations are expressed by:

$$\nabla.\vec{V}_{vel} = 0\,, \tag{1}$$

where $\vec{V}_{vel} = \vec{V}_{vel}(u(x,y,z), v(x,y,z), w(x,y,z))$ is the liquid flow velocity vector.

Using the coordinate system, Eq. 1 can be rewritten as:

$$\frac{\partial u}{\partial x} + \frac{\partial v}{\partial y} + \frac{\partial w}{\partial z} = 0 \tag{2}$$

and the Navier–Stokes equations are given by:

$$\rho\nabla.(\vec{V}_{vel} \otimes \vec{V}_{vel}) = -\nabla p + \mu_{eff}\nabla.(\nabla\vec{V}_{vel} + (\nabla\vec{V}_{vel})^T) + B \tag{3}$$

where p is the pressure, ρ is the density, μ_{eff} is the effective viscosity accounting for turbulence, ⊗ is a tensor product and B is the source term, which is equal to zero for the flow in the stationary components like the diffuser

For flows in an impeller rotating at a constant speed ω, the source term can be written as follows:

$$B = -\rho\left(2\vec{\omega}x\vec{V}_{vel} + \vec{\omega}x(\vec{\omega}x\vec{r})\right) \tag{4}$$

where $\vec{r}$ is the location vector, $2\vec{\omega}x\vec{V}_{vel}$ is the centripetal acceleration and $\vec{\omega}x(\vec{\omega}x\vec{r})$ is the Coriolis acceleration.

Using the coordinate system, Eq. 3 can be rewritten as:

$$\begin{aligned}
\rho\left(u\frac{\partial u}{\partial x} + v\frac{\partial u}{\partial y} + w\frac{\partial u}{\partial z}\right) &= \mu_{eff}\left(\frac{\partial^2 u}{\partial x^2} + \frac{\partial^2 u}{\partial y^2} + \frac{\partial^2 u}{\partial z^2}\right) \\
&\quad - \frac{\partial p}{\partial x} + B_x \\
\rho\left(u\frac{\partial v}{\partial x} + v\frac{\partial v}{\partial y} + w\frac{\partial v}{\partial z}\right) &= \mu_{eff}\left(\frac{\partial^2 v}{\partial x^2} + \frac{\partial^2 v}{\partial y^2} + \frac{\partial^2 v}{\partial z^2}\right) \\
&\quad - \frac{\partial p}{\partial y} + B_y \\
\rho\left(u\frac{\partial w}{\partial x} + v\frac{\partial w}{\partial y} + w\frac{\partial w}{\partial z}\right) &= \mu_{eff}\left(\frac{\partial^2 w}{\partial x^2} + \frac{\partial^2 w}{\partial y^2} + \frac{\partial^2 w}{\partial z^2}\right) \\
&\quad - \frac{\partial p}{\partial z} + B_z
\end{aligned} \tag{5}$$

where $B_x = \rho\left(\omega_z^2 r_x + 2\omega_z v\right)$, $B_y = \rho\left(\omega_z^2 r_y - 2\omega_z u\right)$ and $B_z = 0$.

Furthermore, μ_{eff} is defined as $\mu_{eff} = \mu + \mu_t$, where μ is the dynamic viscosity and μ_t is the turbulence viscosity, it is linked to turbulence kinetic energy k and dissipation ε via the relationship: $\mu_t = C_\mu \rho k^2 \varepsilon^{-1}$, where C_μ is a constant.

The values for k and ε stem directly from the differential transport equations for turbulence kinetic energy and turbulence dissipation rates:

$$\nabla.(\rho\vec{V}_{vel}k) = \nabla.[(\mu + \frac{\mu_t}{\sigma_k})\nabla k] + p_k - \rho\varepsilon \tag{6}$$

$$\nabla.(\rho\vec{V}_{vel}\varepsilon) = \nabla.[(\mu + \frac{\mu_t}{\sigma_\varepsilon})\nabla\varepsilon] + \frac{\varepsilon}{k}(C_{\varepsilon 1}p_k - C_{\varepsilon 2}\rho\varepsilon) \tag{7}$$

where $C_{\varepsilon 1}$, $C_{\varepsilon 2}$ and σ_ε are constants. p_k is the turbulence production due to viscous and buoyancy forces, which is modeled using:

$$\begin{aligned}
p_k &= \mu_t\nabla\vec{V}_{vel}.(\nabla\vec{V}_{vel} + \nabla\vec{V}_{vel}^T) + p_{kb} \\
&\quad - \frac{2}{3}\nabla.\vec{V}_{vel}(3\mu_t\nabla.\vec{V}_{vel} + \rho k)
\end{aligned} \tag{8}$$

$$p_{kb} = -\frac{\mu_t}{\rho\sigma_\rho}g.\nabla\rho \tag{9}$$

where p_{kb} can be neglected for the k-ε turbulence model.

Additionally, for the flow modeling near the wall, the logarithmic wall function is used to model the viscous sub-layer (Ansys inc., 2011).

To solve equations 2 and 5 numerically while accounting for the boundary conditions and turbulence model k-ε, the computational fluid dynamics ANSYS-CFX code, based on the finite volume method, was used to obtain the liquid flow velocity and pressure distributions. Pressure velocity coupling is calculated in ANSYS-CFX code using the Rhie Chow algorithm (Ansys inc., 2011).

In the cases examined involving the pump stage, the boundary conditions were formulated as follows: the static pressure provided was given at the stage inlet, while the flow rate provided was specified at the stage outlet. The frozen rotor condition was used for the impeller-diffuser interface. A no-slip condition was set for the flow at the wall boundaries.

The pump head is determined as follows:

$$H = \frac{p_{to} - p_{ti}}{\rho g} \tag{10}$$

where p_{ti} is the total pressure at the pump inlet and p_{to} the total pressure at the pump outlet as shown in Fig. 2. They are expressed as:

$$p_{ti} = p_i + \frac{\rho}{2} V_{vel_i}^2 \quad \text{and} \quad p_{to} = p_o + \frac{\rho}{2} V_{vel_o}^2 \qquad (11)$$

Moreover, the hydraulic power of the pump is given by $P_h = \rho Q g H$, where Q is the flow rate and H is the pump head.

In addition, the brake horsepower of the pump stage is expressed as $P_s = C\omega$, where ω is the angular velocity and C is the impeller torque.

From the hydraulic power and the brake horsepower, the efficiency of the pump stage can be written as $\eta = \frac{P_h}{P_s}$. It can also be formulated in terms of the hydraulic efficiency (η_h), the volumetric efficiencies (η_v), and mechanical efficiency (η_m) as $\eta = \eta_h \eta_v \eta_m$.

3 RESULTS AND DISCUSSION

The main reference data used for the impeller were 195 mm for the inner diameter, 406 mm for the outer diameter, 6 for the number of blades and 1750 rpm for the rotating speed. For the diffuser, the main reference data were 407.016 mm for the inner diameter, 571.5 mm for the outer diameter, 11 for the number of vanes and 8 for the number of return vanes. The numerical simulation results presented in this work were obtained with the highest accuracy by conducting mesh-independent solution tests in each case study using different numbers of mesh elements.

3.1 Impact of the Number of Impeller Blades

To analyze the impact of the number of impeller blades on the pump stage head, the brake horsepower and efficiency, three impellers with 5, 6 and 7 blades were selected for a diffuser with 11 vanes and 8 return vanes, while the other parameters were kept constant. Fig. 4 shows the head as a function of the volume flow rate, illustrating that the head and the static pressure keep increasing as the number of blades increases. Thus, the ideal head is produced when the number of impeller blades becomes infinite. Additionally, as shown in Fig. 5, the brake horsepower increases relative to the increased number of impeller blades. This is due to the increase in the request pump shaft torque, as the number of impeller blades also increases.

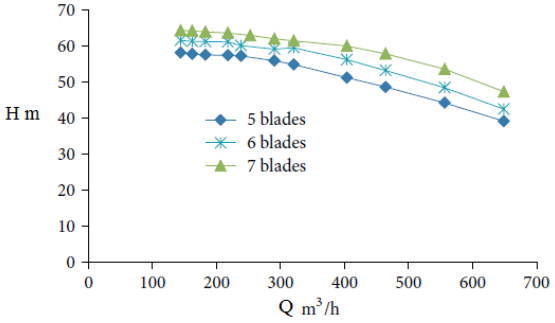

Figure 4: Pump stage head versus volume flow rate.

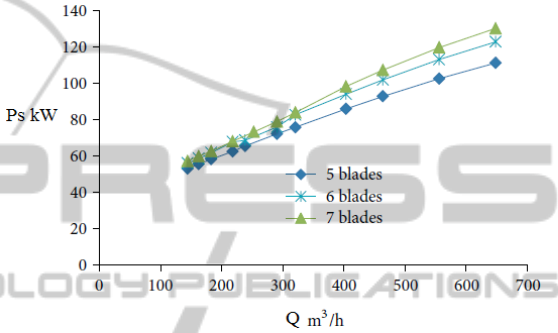

Figure 5: Brake horsepower versus volume flow rate.

Furthermore, Fig. 6 shows the efficiency curves, showing that the impellers with 5 and 6 blades have the same efficiency that is lower than the efficiency for the impeller with 7 blades for large volume flow rates.

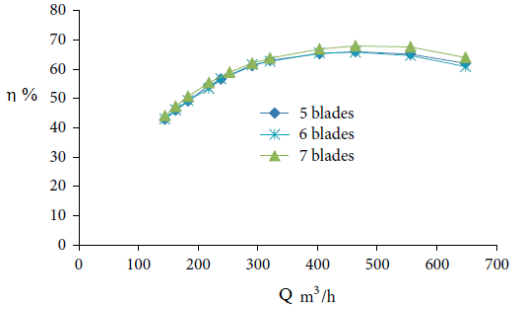

Figure 6: Efficiency versus volume flow rate.

In addition, the distribution of the pressure difference for Q = 464 m^3/h in the impeller, diffuser and diffuser return vane passages is indicated in Tab. 1.

3.2 Impact of the Number of Diffuser Return Vanes

To investigate the impact that the number of diffuser return vanes has on the pump stage head, brake horsepower and efficiency, three diffuser models

Table 1: Distribution of pressure difference.

Blade number	Pressure difference Δp Pa			
	Impeller	Diffuser	Diffuser return vane passages	Δp_{total}
5	476784	98196	-100018	474962
6	512751	108942	-102010	519683
7	547270	120316	-102618	564968

with 3, 8 and 11 return vanes, and 11 vanes were selected considering an impeller with 6 blades, while other parameters were kept constant. Fig. 7 shows the head as a function of the volume flow rate, where it is observed that the head obtained with the 3 diffuser return vanes is the lowest. This can be explained by the fact that the variation in the number of diffuser return vanes affects flow loss due to flow guidance and friction loss in diffuser return vanes. As depicted in Fig. 8, the brake horsepower is only slightly affected by the number of diffuser return vanes.

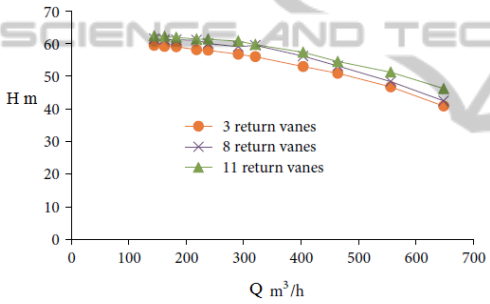

Figure 7: Pump head versus volume flow rate.

Furthermore, Fig. 9 shows that for higher volume flow rates, the efficiency of the diffuser with 11 return vanes is highest. This figure also indicates that the efficiency is lowest for 5 diffuser vanes.

Additionally, Tab. 2 indicates the pressure difference in the impeller, diffuser and diffuser return vane passages, where it can be observed that the highest pressure loss in the diffuser with 3 return vanes.

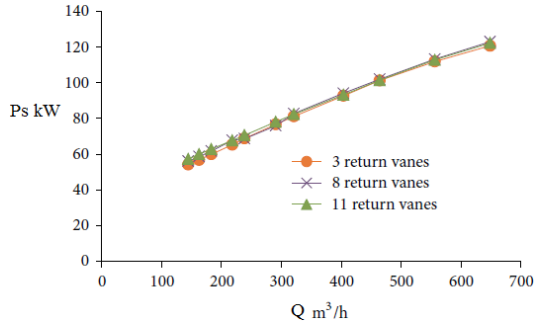

Figure 8: Brake horsepower versus volume flow rate.

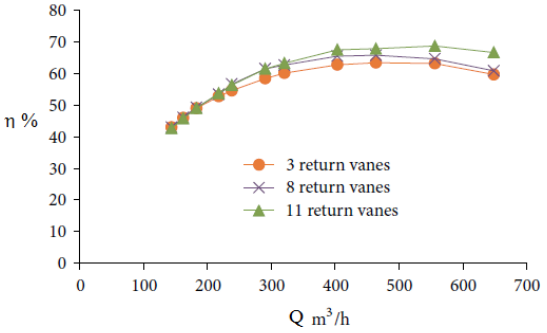

Figure 9: Efficiency versus volume flow rate.

Table 2: Distribution of pressure difference.

Return vane number	Pressure difference Δp Pa			
	Impeller	Diffuser	Diffuser return vane passages	Δp_{total}
3	517349	103444	-122147	498646
8	512751	108942	-102010	519683
11	516752	107500	-92048	532204

3.3 Impact of the Number of Stages

To analyze the impact that the pump stage number has on the pump head, brake horsepower and efficiency, three centrifugal pumps with 2, 3, 4 stages were selected, while the other parameters were kept constant. Fig. 10 represents the head as a function of the volume flow rate, illustrating that the pump head increases as the number of centrifugal pump stages increases.

Moreover, as shown in Fig. 11, the brake horsepower increases relative to the increased number of centrifugal pump stages. This is due to the increase in the request pump shaft torque, as the number of centrifugal pump stages increases.

Furthermore, Fig. 12 indicates that the increase of the number of centrifugal pump stages does not nearly affect the pump efficiency.

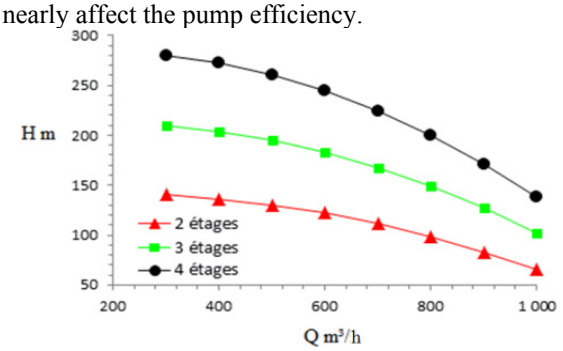

Figure 10: Pump stage head versus volume flow rate.

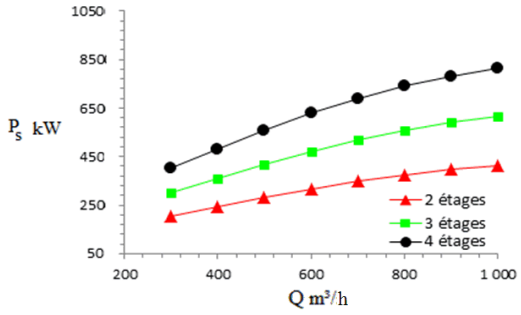

Figure 11: Brake horsepower versus volume flow rate.

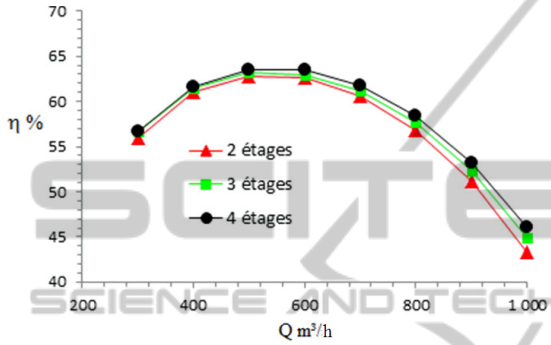

Figure 12: Efficiency versus volume flow rate.

In addition, Fig. 13 represents the corresponding contours for static pressure. There, it can be seen that the static pressure increases with increasing the pump stage number as depicted in Tab. 3

Table 3: Distribution of pressure difference Δp [Pa].

	Number of stages		
	2	3	4
Suction	-45 616	-45 731	-45 850
Stage # 1	575 385	570 477	570 527
Stage # 2	638 616	559 292	556 666
Stage # 3	-	634 570	556 320
Stage # 4	-	-	637 700
Discharge	-87 020	-89 690	-89 090
Δp_{total}	1 081 365	1 628 918	2 186 273

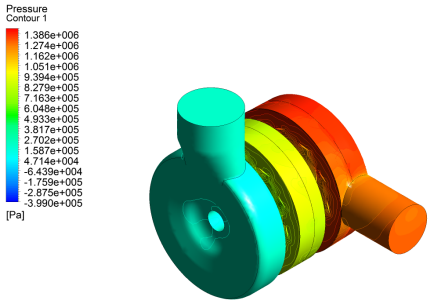

a) 2-stage centrifugal pump

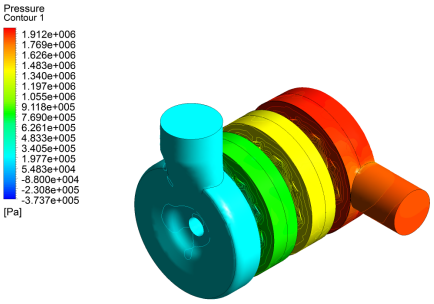

b) 3-stage centrifugal pump

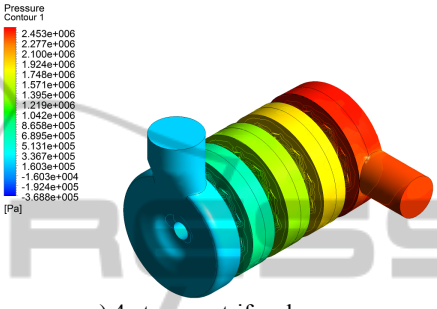

c) 4-stage centrifugal pump

Figure 13: Static pressure contour

3.4 Model Validation

To validate the model developed for the multistage centrifugal pump, the numerical simulation results were compared with the experimental results obtained from Technosub for a first stage. Figs. 14-16 show the comparison between the experimental and numerical curves for the head, brake horsepower and efficiency, respectively. From these figures, it can be seen that there is good harmony between the numerical and experimental results.

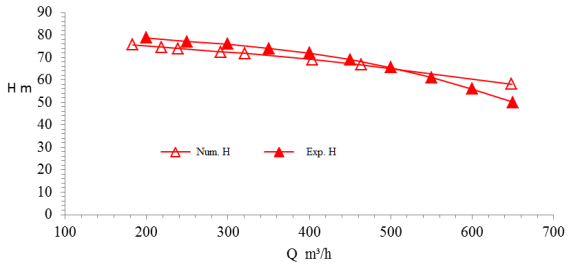

Figure 14: Pump stage head versus volume flow rate.

4 CONCLUSIONS

In this work, a steady state liquid flow in a two-, three- and four-stage centrifugal pumps was numerically investigated. A model of a centrifugal pump stage composed of an impeller, diffuser and casting was developed to analyze the impacts of the

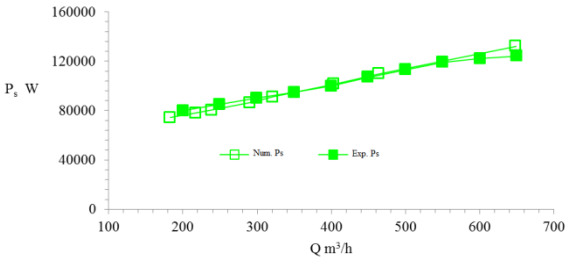

Figure 15: Pump stage brake horsepower versus volume flow rate.

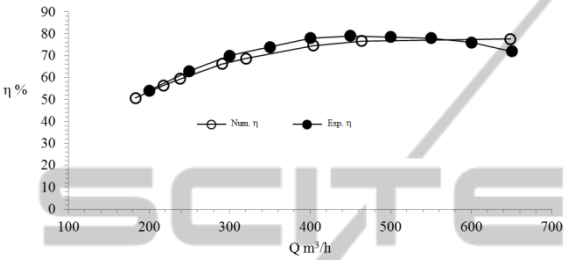

Figure 16: Pump stage efficiency versus volume flow rate.

number of impeller blades, diffuser return vanes and stage on the head, brake horsepower and efficiency of the pump. The results obtained demonstrate, among other things, that the pump stage head and brake horsepower increase as the number of impeller blades increases. Furthermore, the head and efficiency increase for large volume flow rates with increasing numbers of the diffuser return vanes. The brake horsepower hardly varies at all regardless of the number of diffuser return vanes. Additionally, the results obtained clearly reveal that the head and brake horsepower of a multistage centrifugal pump increase as the number of the stage increases. The efficient is less affected by the pump stage number. The comparison of the developed model with the experimental results shows good agreement.

NOMENCLATURE

B	source term (Nm^{-3})
C	torque (Nm)
g	acceleration of gravity (ms^{-2})
H	head (m)
P	power (W)
p	pressure (Nm^{-2})
p_κ	turbulence production due to viscous and buoyancy forces
Q	flow rate (m^3s^{-1})
r	radial coordinate (m)
V	velocity (ms^{-1})
u	flow velocity in x direction (ms^{-1})
v	flow velocity in y direction (ms^{-1})
w	flow velocity in z direction (ms^{-1})
x	x-coordinate (m)
y	y-coordinate (m)
z	z-coordinate (m)

Greek symbols

Δ	difference
ε	turbulence dissipation ($m^2 s^{-3}$),
η	efficiency
κ	turbulence kinetic energy ($kg\ m^{-2}\ s^{-2}$)
ρ	fluid density ($kg\ m^{-3}$)
μ	dynamic viscosity (Pa s)
μ_{eff}	effective viscosity (Pa s)
μ_t	turbulence viscosity (Pa s)
ω	angular velocity ($rad\ s^{-1}$)

Subscripts

1	inlet
2	outlet
h	hydraulic
i	inlet
m	mechanical
o	outlet
s	shaft
t	total
v	volumetric
vel	velocity

ACKNOWLEDGMENTS

The authors are grateful to the Foundation of University of Quebec in Abitibi-Temiscamingue (FUQAT) and the company Technosub inc.

REFERENCES

Peng W. 2008. *Fundamentals of turbomachinery*. Hoboken, New Jersey, John Wiley and Sons.

Huang S., Islam M. F., Liu P. 2006. Numerical simulation of 3 D turbulent flow through an entire stage in a multistage centrifugal pump. *International Journal of Computational Fluid Dynamics,* Vol. 20, Issue 5, Pages 309-314.

Miyano M., Kanemoto T., Kawashima D., Wada A., Hara T., Sakoda K. 2008. Return Vane Installed in Multistage Centrifugal Pump. *International Journal of Fluid Machinery and Systems*, Vol. 1, No. 1.

Kawashima D., Kanemoto T., Sakoda K., Wada A., Hara T. 2008. Matching Diffuser Vane with Return Vane Installed in Multistage Centrifugal Pump. *International Journal of Fluid Machinery and Systems*, Vol. 1, No. 1.

Gantar M., Florjancic D., and Sirok B. 2002. Hydraulic Axial Thrust in Multistage Pumps - Origins and Solutions. *Journal Fluids Engineering*, Vol. 124, Issue 2, 336-341.

Jirout T. 2014. Pumping capacity of pitched blade multi-stage impellers. *Chemical and Process Engineering*, 35 (1), 47-53.

Nicolas La Roche-Carrier N., Dituba Ngoma G., and Ghie W. 2013. Numerical investigation of a first stage of a multistage centrifugal pump: impeller, diffuser with return vanes, and casing. *ISRN Mechanical Engineering*, Volume 2013, Article ID 578072, 15 pages.

Ansys inc. 2011. *ANSYS-CFX (CFX Introduction, CFX Reference Guide, CFX Tutorials, CFX-Pre User's Guide, CFX-Solver Manager User's Guide, CFX-Solver Modeling Guide, CFX-Solver Theory Guide)*, release 14.0, USA.

Technosub Inc., www.technosub.net.